A spontaneous dissociative episode during an EEG experiment

Jamieson, Graham; Cardeña, Etzel; de Pascalis, Vilfredo

Published in:
Brain and Cognition

DOI:
10.1016/j.bandc.2023.106121

2024

Document Version:
Publisher's PDF, also known as Version of record

Brain and Cognition 174 (2024) 106121

Contents lists available at ScienceDirect

Brain and Cognition

journal homepage: www.elsevier.com/locate/b&c

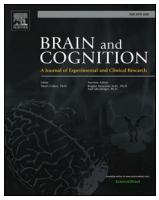

Case Study

A spontaneous dissociative episode during an EEG experiment

Graham Jamieson [a], Etzel Cardeña [b,*], Vilfredo de Pascalis [c]

[a] School of Psychology, University of New England, Australia
[b] CERCAP, Department of Psychology, Lund University, Sweden
[c] Department of Psychology, La Sapienza University of Rome, Italy

ARTICLE INFO

Keywords:
Dissociation
Depersonalization
Ganzfeld
EEG gamma band
Left insula
Sense of self
Predictive coding

ABSTRACT

A depersonalization episode occurred unexpectedly during an electroencephalogram (EEG) recording for a study. Experience reports tracked the time course of this event and, in conjunction, with EEG data, were analyzed. The source activity across canonical frequency bands was analyzed across four periods ended by retrospective experience reports (depersonalization was reported in the 2nd period). Delta and theta decreases occurred across all time periods with no relation to reported events. Theta and alpha increases occurred in right secondary visual areas following depersonalization, which also coincided with surges in beta and gamma. The largest increases occurred in bilateral fronto-polar and medial prefrontal cortex, followed by inferior left lateral fronto-insula-temporal cortices and right secondary visual cortex. A high frequency functional network with a principal hub in left insula closely overlapped inferior left cortical gamma band-power increases. Bilateral frontal increases in gamma are consistent with studies of dissociation. We interpret gamma and later beta, alpha, and theta band increases as arising from the generation of visual priors, in the absence of precise visual signals, which constrain interoceptive and proprioceptive predictions to reestablish a stable sense of physiological-self. Beta showed local increases following the pattern of gamma but showed no changes in functional connectivity.

1. Introduction

This is a single case study of an experimental participant who had a sudden flashback to a near fatal childhood drowning, inadvertently triggered by the experimental (ganzfeld) procedure, and then had a dissociative experience. During it, she reported feeling like a stone and unable to move. The construct of dissociation is complex and includes depersonalization/derealization (DD; a sense of disconnectedness with the body and/or the environment, unwanted intrusions intro awareness, and loss of information or control; Cardeña & Carlson, 2011; Cardeña, Gušić, & Cervin, 2022; Schimmenti & Sar, 2019).

Depersonalization phenomena can be placed within the defense cascade model (Schauer & Elbert, 2010), in which responses to dangerous stimuli of hyperarousal/hypervigilance responses give way to tonic immobility and a psychological sense of disconnectedness, moving from an endocannabinoid to a kappa/mu opiod system. Relatedly, in the neurobiological model of Mobbs et al. (2009), as threat becomes more imminent, neural processing shifts from prefrontal brain regions to subcortical ones involved in primary defense responses (e.g., amygdalae and periaqueductal gray regions), particularly in individuals who have a strong dissociative/overmodulation response to trauma and stressors (Lanius et al., 2018). An example of overmodulation is a study in which patients with depersonalization evinced amygdalae signal decreases in response to more intense emotional images, in contrast with the comparison group, which showed the opposite pattern (Lemche et al., 2008).

Various studies have looked at changes in brain metabolism related to pathological dissociation. Roydeva and Reinders (2021) concluded from a review of 205 studies with diverse brain imaging techniques that dissociation relates to the function of the dorsomedial and dorsolateral prefrontal cortex, bilateral superior frontal regions, (anterior) cingulate, posterior association areas and basal ganglia, with heart rate and other physiological indexes being inconclusive. A few studies have specifically targeted EEG activity in depersonalization disorder or episodes. In a review, Salami, Andreu-Perez, and Gillmeister (2020) concluded that there are EEG biomarkers of depersonalization episodes. In the four EEG studies they listed, a common finding was increased slow brainwave activity, including delta (Locatelli, Bellodi, Perna, & Scarone, 1993) and theta (Hayashi, Makino, Hashizume, Nakano, & Tsuboi, 2010; Raimo, Roemer, Moster, & Shan, 1999) power, but with increases in both alpha and theta in a case study (Hollander et al., 1992).

* Corresponding author.
E-mail address: Etzel.Carden@psy.lu.se (E. Cardeña).

https://doi.org/10.1016/j.bandc.2023.106121
Received 5 September 2023; Received in revised form 14 November 2023; Accepted 15 December 2023
Available online 23 December 2023

More specifically, in Locatelli et al. (1993) panic disorder patients with depersonalization showed increase of slow EEG activity and no responsiveness in the faster alpha frequency band during odor stimulation, a pattern that differed markedly form the panic patients without depersonalization. Also with a sample of panic disorder patients with or without depersonalization, Hayashi et al. (2010) used photic stimulation and hyperventilation to elicit potential repeated trains of theta waves abnormalities than did not (8 vs. 4). In a case study, one episode of alcohol-induced depersonalization (feeling detached, "in a daze") related to an increase in slow wave activity, compared with two asymptomatic episodes (Raimo et al., 1999). Finally, a recent study using exposure to a face mirror as a stressor compared patients with dissociative disorders not otherwise specified with healthy controls and reported a moderate correlation between acute dissociation and higher EEG power at the beginning of exposure , but only four EEG channels were recorded (Schäflein et al., 2022).

With respect to other brain imaging techniques, using positron emission tomography (PET) Simeon et al. (2000) reported that, as compared with a healthy group, patients with depersonalization had lower metabolic activity in right Brodmann's areas 22 and 21 of the superior and middle temporal gyri and higher metabolism in Brodmann's parietal areas 7B and 39 and left occipital Brodmann area 19; and area 7B metabolism correlated with depersonalization measure scores. An fMRI study compared a non-clinical group with patients with conventional PTSD, PTSD dissociative subtype, and DID, and reported that higher scores in dissociation related to less connectivity between middle temporal gyrus and rCEN (clusters 40, 53), and higher connectivity between temporal-parietal-occipital junction and rCEN (cluster 51), in addition to hyperconnectivity in the parahippocampal gyrus (cluster 1, 3, 4) (Lebois et al., 2022).

A few papers have evaluated the relation between cardiac activity and brain connectivity in patients with dissociation. An fMRI study with a patient with a dissociative disorder showed, as compared with controls, decreased performance in a heartbeat detection task (tapping a keyboard in synchrony with the heartbeat along with lower brain connectivity; Sedeño et al., 2014). Heartbeat evoked potentials (HEPs) are interpreted as indicators of cortical representation of bodily signals and they differed between healthy and depersonalization groups during a heartbeat perception task (Schulz et al., 2015). Park et al. (2018) linked heartbeat-evoked potentials (related to insula, operculum, the amygdala, and fronto temporal cortex) to an altered sense of self-identification produced by touch asynchronously matched with video information of the participants' back. Kim and Jeong (2019) found heartbeat synchronized activity in theta but not other brainwaves.

In sum, although some studies have found power or localization EEG differences in particular areas between psychologically healthy individuals or those with depersonalization, there are very few in which EEG activity was recorded during a spontaneous depersonalization/derealization episode. The most consistent finding is an increase in spectral band power in the lower frequency range associated with episodes of depersonalization. However, scalp recorded EEG provides little information about the underlying cortical dynamics or their linkage with the phenomenology of depersonalization.

1.1. The current study

There is a growing body of brain imaging studies related to the important and interwoven phenomena of trauma and dissociation, but these studies focus mainly on the sequelae or chronic conditions related to what are intrinsically dynamic episodes in the life of an individual. The opportunity presented here to map the dynamics of a single episode from onset, through the acute phase, to coping response and resolution posed a considerable methodological challenge. We adopted the following strategy to assess what could be gleaned from the dataset. First, we opted not to test specific hypotheses as this is not supported by the state of the available literature. Rather we sought to map those features of the EEG data salient to the phenomenological reports of the individual and the transition of those reports over a brief 20 min time period. In this case, the data of a single participant could only be compared across time. The methods of group comparison and experimental controls, no matter how desirable, were not available. Having an initial baseline at the beginning of a scheduled experiment we chose to systematically map the changes from that baseline in cortical source activity of the canonical EEG frequency bands across the successive time periods for which experience reports were available, focusing on the time periods immediately prior to each corresponding report. We used a nonparametric statistical approach with minimal assumptions to map these features (Nichols & Holmes, 2002). In order to interpret these features, we are guided by the principles adopted in single case study behavioral designs that seek to identify discrete patterns in the time series of observations. In particular, we identify and interpret a series of observations in which there is: no change across time; an observed change only at the time point of a critical event (in this the report of acute depersonalization), and a persistent change following the time point of the event of interest (Cooper, Heron, & Heward, 2020).

2. Materials and methods

2.1. Participant

While conducting an EEG study on states of consciousness using a sensory homogenization procedure, a participant unexpectedly reported anxiety and then dissociative phenomena after an unexpected memory of her drowning as a child was evoked by exposure to pink noise. Participant Z was a right-handed (according to the EHQ, see below) woman in her 40 s recruited for an EEG ganzfeld/hypnosis experiment. She did not report psychological distress before the experiment (according to the BSI, see below), is highly hypnotizable (according to the HGSHS and the SHSS:C, see below), and reported non-clinical levels of trait dissociation (according to the DSS, see below). She gave informed consent for the study, which was approved by Sweden's Ethic Board (#2016-243), and reiterated her approval for us to use her data at the end of her session.

2.2. Measures

The *Brief Symptom Inventory* (BSI; Derogatis, 1975) is a widely used measure of psychological distress. We did not score its various subscales but used it only to screen out potentially distressed participants. Z did not report noticeable distress when responding to this scale in a session before the experimental one.

The *Dissociative Symptom Scale* (DSS; Carlson et al., 2018) is a valid and reliable measure of trait dissociation with 20 items each with anchor points between 0 and 4. Z had a score of 12, lower than scores for clinical samples (cf. Carlson et al., 2018).

The *Edinburgh Handedness Questionnaire* (EHQ; Oldfield, 1971) is a valid and reliable measure of hand preference for different tasks (e.g., writing, using a broom). Z scored 100 % as right handed.

EEG recording. To reduce possible noise from metal in earphones, we used an EchoTubeZ Radiation free air tube headset. EEG was recorded with an EasyCAP electrocap using SynAmps2 amplifiers.

The *Harvard Group Scale of Hypnotic Susceptibility* (HGSHS; Shor & Orne, 1962) is a group measure of hypnotizability with good psychometric measures, consisting of a relaxation induction followed by 12 suggestions of increasing difficulty. Z scored as a "high hypnotizable," passing 10 suggestions.

The *Stanford Hypnotic Suggestibility Scale: C* (SHSS:C; Weitzenhoffer & Hilgard, 1962) is a more demanding measure than the individual measure of hypnotizability (Council, 1999) and consists of a relaxation induction and 12 suggestions of increasing difficulty. Z corroborated her status as a "high" hypnotizable, with a score of 9 or higher (after passing 9 items the administration of the Scale was discontinued).

The *Subjective Experiences Scale* (SES) (Kirsch, Council, & Wickless, 1990) is a 12-item questionnaire with a five-point response format that measures experiential involvement for each HGSHS suggestion. Higher scores reflect greater involuntariness and experiential involvement during hypnosis and Z had a very high score of 44.

2.3. Procedure

Z was participating in an EEG neurophenomenological study comparing two different procedures: ganzfeld (a sensory homogenization procedure in which the person is exposed to unchanging red light through translucent googles and pink noise, while sitting in a comfortable chair; cf. Wackermann, Pütz, & Allefeld, 2008), and hypnosis (which Z did not get to experience because her participation was discontinued after the ganzfeld session). For the first and only session, we placed the electrocap and lowered the impedance while she responded to handedness and dissociation scales. We explained to her that every few minutes (5 on average), we would ask her how altered she felt her consciousness was according to a scale from 0 (wide awake)-10 (as altered as could get), and what she had been experiencing just before the probe, a method used by one of us in previous studies (e.g., Cardeña, 2005; Cardeña, Jönsson, Terhune, & Marcusson-Clavertz, 2013).

We initiated the session with a 2 min baseline for which she was just asked to relax while keeping her eyes open. At the end of the baseline, she responded that her state was 0 (i. e., not altered at all) and she had just been calm and relaxed. Then we set her up with translucent ovals covering her eyes, a red light in front of her, and earphones that played pink noise. She heard through the earphones 4 min of relaxing instructions, asking her to keep her eyes open, followed by 4 min of ganzfeld exposure. At the end of this period, she stated that her state was 4 (in the scale from 0 to 10) and reported: "I don't see the red light it's black. It feels as if I am drowning, I am in water."

Because this was an unusual response in our experience and one that was distressing, we asked her whether she was fine and whether she was scared, to which she responded that she was not scared and that "yes, I'm not struggling or anything."

Given these reassurances, we continued with the experiment. After 5 min more she responded that her state was 5 and that she was "all in my head and not at all in my body. I feel dry and I can see a beach house." At the next probe after 5 min more, she responded that her state was 5 and that she was "Stiff and a bit cold, as if I can't move. It feels as if I cannot move, I feel like a stone, cannot move, cold, my left eye is sort of twitching, a sensation in the physical body."

Five minutes later she again reported a state of 5 and that she had "A bit of anguish, sort of it feels like I'm in between being awake and asleep and there is a threat or menace somewhere, feel a bit afraid or worried." We then asked her whether she could continue to which she responded yes, but a few minutes later she asked if we could stop, which we proceeded to do immediately.

While trying to comfort her while taking off the electrode cap, she mentioned "Feeling dizzy, as if I could faint. Felt very warm, sweaty (she was very sweaty), used to faint when I was younger. I felt as if I was losing control." And then mentioned that she had almost drowned as a child, and the pink noise had reminded her of that. It is important to note that no other participant in the study discontinued or reported either depersonalization or distressing experiences.

2.4. Analyses of the EEG

2.4.1. EEG data acquisition

Electroencephalogram (EEG) was recorded using a 64 channel Neuroscan QuikCap with sintered Ag/AgCl electrodes. EEG recordings from 62 electrode sites were employed in the current study. These cap electrodes were positioned at sites LIST as described by the international 10/20 system. The ground electrode was located at AFz and the recording reference midway between electrodes Cz and CPz. Cap electrodes located at M1 and M2 were not included in this study. EEG signal was acquired using a Synamps2 24-bit digital amplifier at a sampling rate of 500 Hz with a recording filter of DC to 250 Hz and recorded with Curry 7 acquisition software. Impedance levels were below 5 kΩ at the before recording.

2.4.2. EEG preprocessing

Following visual inspection, the recording was interpolated for electrodes CP4 and FT9. A 2nd order Butterworth bandpass filter of 0.5–60 Hz was then applied converting the recording to a common average reference. Five recording segments of 120 s each were then extracted for analysis. The first 120 s segment of the recording (corresponding to the relaxation instruction period) served as the Eyes Open (EO) baseline for subsequent comparisons. The remaining recording segments were extracted for each of the 120 s periods prior to the event marker for the beginning of each of the 4 consecutive experience probes (P1, P2, P3 and P4) delivered during the ganzfeld session.

These recording segments were concatenated and we performed automated ICA artifact correction using FASTER-ICA (Nolan, Whelan, & Reilly, 2010) using standard settings for artifact component identification. By removing components displaying exceptionally high changes in median gradient, Hurst exponents, filter band slopes, and spatial kurtosis the FASTER algorithm is effective at identifying components associated with a broad range of artefact types.

Following artifact correction with FASTER, the file was again referenced to common average and split into its 5 constituent segments. Each of these segments was further divided into 10 s epochs for further analysis. A final visual inspection was performed to exclude any epoch containing obvious eye or other remaining movement artefacts. This resulted in 11 available epochs for EO baseline, P1, and P4 and 12 available epochs for P2 and P3.

2.4.3. Source analysis

Source localization estimates of EEG frequency band activity were obtained for delta (0.5–4 Hz), theta (4 – 8 Hz), alpha (8–12 Hz), beta (12–30 Hz) and gamma (30–60 Hz) for each available epoch in conditions EO, P1, P2, P3, and P4 using The Key Institute eLORETA (exact low resolution brain electromagnetic tomography; Pascual-Marqui et al., 2011) software,. This technique provides a single weighted minimum norm solution to the inverse problem and hasdemonstrated zero error (but low spatial resolution) in localizing cortical grey matter test sources even in the presence of structured noise (Marco-Pallarés, Grau, & Ruffini, 2005; Pascual-Marqui, 2002). Cortical source activity for the recording periods were identified by computing the three-dimensional distribution of current source density (see Pascual-Marqui, 2009; Pascual-Marqui et al., 2011) in 6,239 5 mm^3 cortical grey matter voxels. The weights utilized by eLORETA yield images of current density in a standardized realistic head model (Fuchs, Kastner, Wagner, Hawes, & Ebersole, 2002) based on the MNI152 template (Mazziotta et al., 2001).

Voxel source activity in the canonical frequency bands were compared between EO baseline and each of P1, P2, P3, and P4, and significant increases and decreases were identified. This enabled a systematic sequential mapping of local cortical changes in each frequency band as they unfolded across the reporting periods, locating them with respect to the depersonalization (before, during, and after) at the end of P2.

2.4.4. Connectivity analysis

We used the results of the spectral band power analyses to identify frequency bands with temporal power increases around P2. Activity in these frequency bands was subject to network connectivity analysis to identify potential functional networks associated with the experience of depersonalization at the end of P2.

Gamma band functional connectivity in P2 was calculated between the centroids of each Brodmann area, a total of 84 ROI, using the lagged non-linear coherence measure (Pascual-Marqui, 2007) implemented in

eLORETA . Lagged non-linear connectivity removes the effects of instantaneous volume conduction that otherwise inflates electrocortical connectivity measures to give a measure of reciprocal (non-linear) signal interactions mediated by (time-lagged) neural transmission. Non-linear connectivity was chosen over its linear counterpart because linear coupling between oscillators fails to capture the emergent (integrated) system dynamics that characterize the form of information in conscious experiences (Brown, 2009; Vinck et al., 2023). Finally, an essentially similar functional connectivity analysis was carried with respect to the beta band in P2.

2.4.5. Statistical analysis

Each available epoch was treated as an individual observation. We compared the EO baseline and each of the P1, P2, P3, and P4 recording periods to track cortically localized bandpower changes in each of the canonical EEG frequency bands as the participant's reported experience progressed from initial calm, the memory of drowning, being cut off from their body (with images of safety), to feeling frozen and immobilized, and finally to the presence of a personal menace. Statistical analyses of changes across all frequency bands and all cortical grey matter voxels were performed simultaneously using random permutation testing (Nichols & Holmes, 2002). Randomization testing is a nonparametric method used to determine p values while simultaneously controlling for family-wise error rate across multiple voxels and frequency bands. For each comparison, a t-test statistic (or pseudo-statistic as it is no longer acting as a parametric statistic) was first calculated at each source voxel (the obtained statistic) for each frequency band. This process was then repeated for 5,000 random reassignments of the data sets to the analysis conditions in order to estimate the distribution of the max voxel statistic (the maximum test statistic value across all voxels in each frequency band) under the null hypothesis that there is no difference between conditions. This distribution is used to provide the significance thresholds and exact p values of the obtained test statistic at each voxel in each frequency band while simultaneously controlling for the family-wise error of multiple voxel and frequency band testing. This nonparametric method requires no assumptions about the data distribution and so may be applied even when assumptions related to the initial test statistic are not met. A corresponding analysis was also performed for EO baseline versus the (focal) P2 recording period for lagged-nonlinear connectivity measure between each pair of ROI to identify significant changes in gamma band and beta band functional connectivity associated with the reported experience of acute depersonalization.

3. Results

3.1. Localization of spectral band power changes across sequential reporting periods

Localized band power in each of the frequency bands (delta, theta, alpha, beta and gamma) were compared at each cortical grey-matter voxel mapped by eLORETA for the recording of the initial eyes open (EO) baseline (calm and relaxed) segment and each consecutive recording period preceding each of the available ganzfeld experience reports: P1 (traumatic recollection), P2 (nonexperience of body, imagery of safety), P3 (cold, numb, unable to move), and P4 (threatening presence, sense of menace, which led to the participant terminating the experiment shortly afterwards). After correcting for family-wise error rate for simultaneous testing across all voxels at all frequency bands, the threshold for significance for an individual test at each voxel was further set to a conservative p <.01 two tailed. The overall pattern of those results is first summarized by reporting the maximum significant voxel difference in each test. Table 1 presents the absolute maximum voxel test statistic, the equivalent Cohen's d, the left or right Brodmann Area, and the MNI coordinates of the voxel. Table 2 reports the additional max-voxel statistics that were also significant but in the opposite direction, to those reported in Table 1.

Table 1
Absolute Max-Voxels for each Comparison in each Frequency Band.

	EO v P1	EO v P2	EO v P3	EO v P4
δ	t = 19.0 (d = 4.2) R BA7 25–60 −45	t = 18.5 (d = 4.0) R BA 7 25–60 −45	t = 15.6 (d = 3.4) L BA34 −20 0–15	t = 14.7 (d = 3.3) R BA7 25–60 50
θ	t = 12.0 (d = 2.7) L BA29 −55–70 10	t = 9.8 (d = 2.1) L BA40 −55–55 −25	t = 10.6 (d = 2.3) L BA39 −30–60 25	t = 8.9 (d = 2.0) L BA40 −55–55 25
α	t = 12.2 (d = 2.7) L BA22 −50 75 10	t = 7.3 (d = 1.6) R BA40 55–35 40	t = -7.2 (d = -1.6) R BA18 25–85 −15	t = -7.2 (d = -1.6) R BA17 20–85 0
β	t = 8.9 (d = 2.0) L BA40 −50–50 20	t = -24.7 (d = -5.4) L BA21 −55 10 25	t = -8.2 (d = -1.8) R BA17 15–95 −15	t = -10.0 (d = -2.2) L BA13 −40 20 5
γ	t = -7.7 (d = -1.7) L BA10 −40 45 15	t = -36.2 (d = -7.9) Midline BA32 0 35 20	t = -10.9 (d = -2.4) R BA17 15–85 5	t = -14.0 (d = -3.1) R BA18 15–55 15

Note: Positive t values indicate EO > P and negative t values indicate EO < P. Threshold for a large effect size is Cohen's $d \geq 0.8$. L = left, R = right BA = Brodmann Area.

Table 2
Summary of Significant Max-Voxels in Opposite Direction to Absolute Max-Differences.

	EO v P1	EO v P2	EO v P3	EO v P4
δ	_	_	_	_
θ	_	_	t = -7.02 (d = -1.5) R BA19 25–80 20	t = -8.4 (d = -1.9) R BA19 25–75 −20
α	_	_	_	_
β	_	_	_	_
γ	t = 6.7 (d = 1.5) R BA47 30–25 15	_	_	_

Note: Positive t values indicate EO > P and negative t values indicate EO < P. Threshold for a large effect size is Cohen's $d \geq 0.8$. L = left, R = right, BA = Brodmann Area.

Table 1 shows that there were significant changes in localized spectral band power in each of the frequency bands from the EO baseline to the recording segments preceding each of the successive experience reports. In the case of delta there is always a decrease from the preganzfeld baseline and the magnitude of the maximum decrease is similar across each reporting period. The consistent pattern of these changes does not show evidence of a reaction to the unique depersonalization event reported in P2. In the theta band significant max-voxel decreases from baseline also occur in every reporting condition, with a similar high magnitude in each condition and always in the left hemisphere. However, these changes do not appear to be related to the depersonalization event reported in P2.

In the case of the alpha band there are also significant decreases in localized cortical activity from EO to P1 and P2 but in both P3 and P4 (following P2 – the acute depersonalization report) there is now a significant increase in alpha specifically in the right occipital cortex (BA 17/18/19). It is noteworthy that in Table 2 below we see the same temporal and spatial pattern for significantly increased localized theta band activity compared to baseline. Fig. 1 shows the cortical surface projection of significant local increases (shown in blue) in theta and alpha band power in these extrastriate visual regions of right occipital cortex following but not preceding the report of acute depersonalization.

EO v P2

EO v P3

EO v P4

Fig. 1. Inferior Right Hemisphere View of Significant Theta, Alpha, Beta, Gamma Band Power Changes from Baseline to P1, P2, P3 and P4. **Note.** Panels present, from left to right significant theta, alpha. Beta and gamma band changes. Yellow = decrease, Blue = increase. Occipital cortex at top, prefrontal cortex at bottom of each panel. (For interpretation of the references to colour in this figure legend, the reader is referred to the web version of this article.)

Note also that beta and gamma band increases from baseline are also observed in these same regions following P2. Beta and gamma bands uniquely show further patterns of localized increase found only in P2.

3.2. The higher frequency bands: Gamma and beta

Table 1 shows a unique surge in high frequency activity specific to the recording period immediately prior to the second experience report, in which detachment from the body depersonalization is experienced.

This response is clearest and strongest in gamma where the max-voxel statistic for power increase in P2 reaches an effect size almost ten times the threshold for a large effect. Significant voxel changes are first summarized globally by cerebral hemisphere for all reporting periods and then broken down according to Brodmann area to depict the unique surge in gamma activity in the P2 reporting period. The total number of significant voxel increases from EO baseline for each reporting period are presented in Table 3 below. Significant gamma band decreases occur only in P1 for a small number of voxels: 10 voxels in the left hemisphere, 1 midline and 3 in the right hemisphere.

Even at this coarse level of granularity it is evident that each of the successive reporting conditions demonstrate a highly distinctive pattern of localized gamma-band power changes. P1 is marked by limited decreases and increases in gamma band power. P2 (which coincides with the reported onset of depersonalization) is marked by a widespread increase in gamma-band power incorporating about one third of all cortical grey matter voxels. This is bilateral but predominantly in the left hemispheres. P3 (the immediately following time period) is marked by a decrease in gamma-band power across most (but not all) voxels significantly activated in P2 but especially so in the left hemisphere. P4 remains similar to P3 but with increasing gamma power in left hemisphere voxels accompanying marked increases in negative affect.

Spectral band-power results show that a pronounced gamma event has occurred in P2 coincident with the depersonalization episode and appears to be resolving in P3 but may have begun building before the participant's decision to terminate the testing session. A similar but less intense pattern of temporal change is observed in the beta band. Consequently, detailed analyses of gamma-band and beta-band changes (band-power and functional connectivity) between EO baseline and P2 were undertaken and are presented below.

Significant changes in gamma band power between EO baseline and P2 are presented, summed by Brodmann area in Table 4 above. Changes in that table may be grouped in 3 categories: Bilateral increases (evident in BA10, BA11, BA24, BA32, and perhaps BA9); left hemisphere only BA increases (most evident in left BA13, left temporal and left inferior frontal regions); increases in visual cortical regions (BA17, BA18, BA19). Cortical views of these changes are rendered in Fig. 2.

4. Gamma-band lagged nonlinear connectivity changes

Differences in lagged nonlinear gamma band connectivity, calculated between centroids of all Brodmann Areas were compared between EO baseline and P2. Twenty connections between 15 ROI (BA centroids) showed significant increases in lagged nonlinear gamma-band connectivity from EO baseline to period P2, all located in the left hemisphere. Because of the nature of the analysis (testing for expected increases in a frequency band), connectivity changes were evaluated at the threshold for $p < .05$ one tailed. Significant connections are presented for internal and external lateral views of the left cortical hemisphere in Fig. 3 below.

A list of all ROI with significant connectivity changes and the number of significant changes is presented in Table 5 below, which shows the left insula (BA13) to be the major hub for gamma-band connectivity increases during P2 with secondary hubs in left Superior temporal gyrus (BA22) and left Postcentral gyrus (BA43).

Although we focused on connectivity increases, it should be mentioned that there were no significant connectivity decreases between ROI in this comparison. It is noteworthy that, with only 1 exception (BA25), all ROI showing connectivity increases form a subset of those BA in Table 4 with voxels showing left, rather than bilateral or right hemisphere, increases in gamma in P2. These gamma results were uniquely identified with the experience reported in P2 time . In summary, the lagged nonlinear connectivity analyses shows a left sided network of gamma-band functional connectivity increases, with the principal hub located in left insula, uniquely associated with P2 and the dissociation triggered at that point.

In beta, power increases also occured with unique intensity and localization in P2 . Comparison of beta band and gamma band results in Table 1 and Table 4 show that these beta changes always and only occurred in the same regions as gamma changes but with reduced intensity and spatial extent. Unlike gamma, there were no significant beta increases in lagged nonlinear functional connectivity in EO versus P2. There was a single connection where the increase reached $p < .10$ between left BA33 (Anterior Cingulate) and left BA17 (Lingual Gyrus). Localized beta band changes uniquely associated with P2 appear in a subset of regions showing corresponding gamma band changes, but increased functional connectivity between these regions were observed only for gamma .

Table 3
Significant Gamma-Band Voxel Increases (p <.01).

	EO v P1	EO v P2	EO v P3	EO V P4
Left Hemisphere	10	1481	22	494
Cortical Midline		37	15	25
Right Hemisphere		436	129	198

Table 4
Significant Voxel Gamma-Band and Beta-Band Power Increases from EO to P2 by Brodmann Area.

	Gamma			Beta		
	Left	Midline	Right	Left	Midline	Right
BA 1	3			1		
BA 2	5					
BA 3	7			2		
BA 4	14			7		
BA 6	55			17		
BA 8	10					
BA 9	117	9	43	16	3	13
BA 10	136	2	134	122	2	108
BA 11	113		94	105		72
BA 13	117			82		
BA 17		2	34			
BA 18		10	52			
BA 19	19		7	3		
BA 20	109			99		
BA 21	105			105		
BA 22	80			75		
BA24	13	6	12	5	2	5
BA 25	7		5	3		1
BA 27	2					
BA 28	20			10		
BA 32	46	6	44	30	5	33
BA 33	1	2	1			
BA 34	16			8		
BA 35	11			4		
BA 36	26			17		
BA 37	86			34		
BA 38	76			76		
BA 39	8					
BA 40	35			4		
BA 41	27			17		
BA 42	19			14		
BA 43	14			14		
BA 44	28			27		
BA 45	29			27		
BA 46	20		6	10		
BA 47	107		4	105		

Note. This table does not take into account total number of voxels in each Brodmann area. Areas without significant voxel changes are not listed.

5. Discussion

This case study examined EEG recorded in conjunction with consecutive experiential reports gathered before, during, and after the emergence of an acute episode of depersonalization inadvertently triggered by associations with a traumatic life event. Immediately prior to the EO baseline period, the participant reported being calm and relaxed.

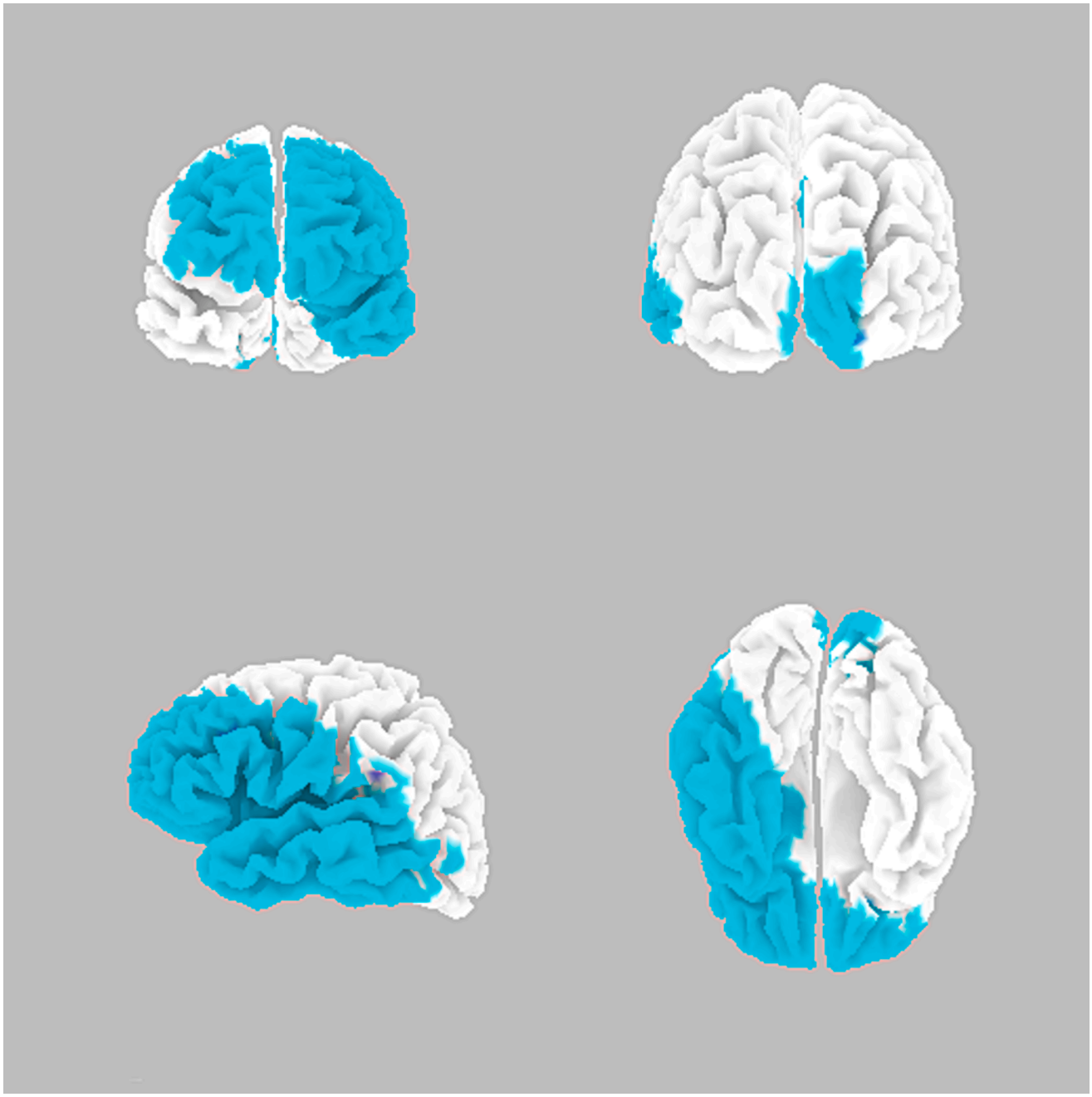

Fig. 2. *Cortex Views of Significant Gamma-Band power Increases from Baseline to P2.* Note. Blue = significant increase. Yellow = significant decrease. Cortical views clockwise from top left: Front; rear; inferior; left lateral. (For interpretation of the references to colour in this figure legend, the reader is referred to the web version of this article.)

In the first reporting period (P1) she appeared to vividly experience a childhood memory of drowning. Her report in P2 then describes the onset of an episode of acute depersonalization in which she experiences herself not as outside of her body but as completely detached from her body imagining a safe place. In the remaining reports awareness of her body and feelings begin to return. These included negative and personally threatening emotions and she elected to discontinue the experiment. The analyses reported here sought to differentiate those changes in the EEG corresponding to core features of this, sudden episode of acute traumatic depersonalization, those that might have been consequences of this event, and those unrelated to this sequence of events.

The present case study, necessarily limited in the available data, sought to systematically explore cortical source activity in the canonical frequency bands. Similar decreases in delta and theta band cortical activity across all time periods point towards a process linked to the experimental condition (ganzfeld) rather than the specific experiences reported in this case study. Increases in activity in right BA17/18/19 across theta, alpha, and beta bands following (but not before or during) the episode of acute depersonalization reported in P2 are plausible features of a subsequent neuropsychological response to regain control following that episode. The most consistent feature with the instantiation of the acute depersonalization episode itself was the surge in gamma activity and functional connectivity unique to P2 and the associated surge in localized beta band activity.

Having identified this gamma event as the clearest feature of the EEG recording distinguishing the onset of acute depersonalization, we sought to describe and interpret the features of these cortical changes in the

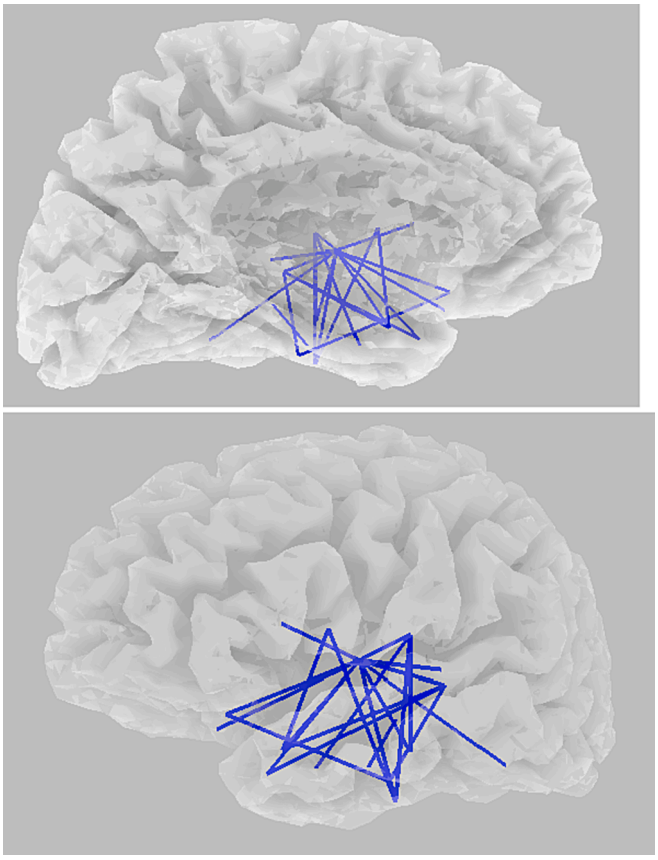

Fig. 3. *Significant Increases in Lagged Nonlinear Gamma-Band Connectivity from EO to P2*. Note. Sagittal and lateral views. Significant increases only in left hemisphere.

Table 5
Significant Gamma-Band Lagged Nonlinear Connectivity Increases for ROI from EO to P2.

Region of Interest (Centroids)	Significant Connections	Anatomical Description
L BA13	11	Insula
L BA20	3	Inferior temporal gyrus
L BA21	2	Mid temporal gyrus
L BA22	4	Superior temporal gyrus
L BA25	1	Subgenual anterior cingulate
L BA28	1	Hippocampal area 1
L BA34	3	Hippocampus
L BA36	2	Parahippocampal gyrus 2
L BA37	1	Occipital-temporal
L BA38	2	Temporal pole
L BA41	1	Primary auditory
L BA43	4	Postcentral gyrus
L BA44	2	Opercular inferior frontal gyrus
L BA45	1	Inferior frontal gyrus
L BA47	2	Ventrolateral prefrontal cortex

Note: BA = Brodmann Area, L = left.

organization of gamma-band activity in P2 . The strongest gamma power increases in this time period are observed in bilateral prefrontal (BA10, BA11) and medial prefrontal (BA32, BA 24) cortex. The next set of cortical regions showing significant increases in gamma-band power are left lateralized and located along or immediately adjacent an inferior horizontal band stretching across the left inferior frontal gyrus, left insula, and left temporal lobe. These regions closely overlap those that comprise the gamma functional connectivity network unique to this recording period. These regions are intermediate in the magnitude of gamma power increases with the final set of regions in visual cortex (BA17, BA18 and BA19) showing significant (albeit the weakest) gamma increases in P2.

Analysis of lagged nonlinear connectivity identified a unique left lateralized gamma-band functional network in P2 with the insula (left BA13) as the principal hub. ROI included in this network were located in left lateral and (interestingly) medial regions of the prefrontal cortex, insula, and temporal lobe. Of note is the smaller connectivity hub in left BA43, which may be somatosensory cortex for sensations generated within the ear (cf. Renaud, 2015). Equally noteworthy is the lack of significant connectivity changes between the ROI in this network and ROI corresponding to any of the other significant localized changes in gamma-band power during P2. Although beta band activity also uniquely surged in P2 in regions associated with the surge in gamma , these changes remained localized. Beta in fact did not show any pattern of increased functional connectivity during the episode of acute depersonalization.

Considerable caution is warranted in any comparison of results from spectral band-power activity in the EEG and metabolic activity recorded in fMRI. There is however, consistent evidence that localized cortical BOLD response is to some extent correlated with increased gamma-band activity in those regions (Herrmann & Debener, 2008; Lachaux et al., 2007; Scheeringa et al., 2011). With this caveat we make the following comparisons.

The strongest finding reported by Roydeva and Reinders (2021) was of increased activity in bilateral dorsomedial, superior frontal, and anterior cingulate cortices in conjunction with pathological dissociation. Our results show a surge in gamma activity in association with an episode of acute traumatic dissociation. The regions in which this response is strongest directly correspond to the bilateral cortical regions of activation identified by Roydeva and Reinders. It should be noted that the observed effect size for the increase in gamma power in these regions in the current case study is of extraordinarily large magnitude, justifying its selection as the most significant electrophysiological feature linked to the reported experience of traumatic depersonalization. We tentatively propose that this gamma event, strongest in these regions, is functionally associated to the similar metabolic activation findings summarized by Roydeva and Reinders.

Both Lanius et al. (2010) for traumatic dissociation, more generally, and Reinders et al. (2014) for identity related dissociation, in particular, have proposed that such prefrontal activation is associated with functional inhibition of activity/response of the amygdalae in response to traumatic events. Such an interpretation is beyond the scope of our study to confirm due to the difficulty of detecting electrophysiological activity from the amygdalae in scalp recorded EEG. However, these frontal regions have rich structural connections with the amygdalae and have been demonstrated to suppress dysfunctional emotional responses by inhibiting the responsiveness of the amygdalae (Etkin, Egner, & Kalisch, 2011). Consistent with this interpretation, our results showed no significant increase in gamma functional connectivity between these prefrontal regions of maximal gamma power increase and any other cortical regions showing significant gamma increases (nor indeed any other cortical region per se). Insofar as this phenomenon is functional (and it may not be), that function is likely to engage functional connections with subcortical rather than cortical brain structures. This absence of accompanying changes in cortical functional connectivity is a feature that must be explained by any final account of this phenomenon.

We expect that the functional network that became activated in P2 most likely plays a wider functional role that extends beyond this case study. Understanding of this network then is important not only for the current case study and the phenomenon of acute dissociation but possibly contributes to further knowledge of currently studied functional brain networks, their fractionation, and their interplay. It is clear that the central hub of this network lies within the left insula. The posterior insula is the primary sensory cortex for interoceptive sensory inputs (Craig, 2010), while the mid insula integrates these signals with

inputs from visual, proprioceptive, and somatosensory processing streams and the anterior insula is a principal hub in the Salience Network with a major role in regulating the Default Mode and Dorsal Attentional Networks and their interplay (Molnar-Szakacs & Uddin, 2022), but the current network does not map in any simple way onto this scheme. Although much is known of the shared functions of the insula, its subregions, and their connections, and of the specific functions of the right insula, relatively little is known of the specific functions of the left insula and it is these that are implicated in the current results. Craig (2005) has proposed that the right insula is specialized to receive interoceptive inputs arising from activity of the sympathetic nervous system and subsequently for the allostatic regulation of the physiological states giving rise to those inputs. He further proposes that the left insula plays a parallel role for the parasympathetic nervous systems and that these functional differences between left and right insula are further integrated with the cognitive-affective specializations of the respective cerebral hemispheres. Biduła and Króliczak (2015) also propose that functional and structural asymmetries in left and right insula may be linked to right and left hemispheric specialization for speech and gesture respectively.

As noted above, there appears to be a close overlap between BA showing left lateralized increases in gamma power and BA centroids (used as ROI) that appear as nodes in the P2 specific left lateralized functional network identified here. Among the regions with left lateralized gamma-band increases, the strongest voxel increases were found in the insula (more specifically the left anterior insula), followed by voxels in left inferior frontal gyrus (BA 47) and then left temporal pole (BA38).

We note that each of these local maxima lie in close proximity to the three principal hubs of a functional network recently identified by Kim and Jeong (2019) in which connectivity is evoked by interoceptive feedback from the heart beat during a task that requires cognitive-affective processing. They termed this discovery the Heart Evoked Network (HEN). They fractionate this network into 3 components, the core being a subcomponent of the Salience network and 2 additional networks each of which is a subcomponent of the Default Mode Network. Taken together, the current functional connectivity results and left lateralized gamma power increases appear to substantially overlap the HEN. We tentatively suggest that current results are related to changes in this as yet little explored network. However, this hypothesis has not been systematically explored in the current findings.

Activity in the insula and the somatosensory cortices show the earliest cortical responses, believed to be generated by interoceptive and proprioceptive feedback respectively, time locked to the contraction (and/or relaxation) of the hearts' ventricles as part of the HEP (Park & Blanke, 2019). Additional cortical responses during the HEP have been linked to sentient or feeling self ("me") mentation in the ventromedial hub of the DMN and narrative self ("I") mentation in the posterior parietal hub of the DMN (Babo-Rebello, Richter, & Tallon-Baudry, 2016). The anterior insula is also a principal hub in the Salience Network, with a major role in regulating the DMN and the Dorsal Attentional Network; it may be important that those functional connections do not appear to be engaged in the current network. We theorize that both the left lateralized increases in gamma power and the left lateralized gamma connectivity network in P2 are driven, if not initiated, by gamma band events in the left insula. The questions which then arise are: why the insula, why the left insula, and why the gamma band?

We propose that this network has abruptly undergone a (temporary) loss in the facility to predict, and thus control (Barrett & Simmons, 2015), sources of interoceptive signals (which may include the heartbeat) critical to what may be called the physiological sense of self, the stability of which is a necessary foundation for the ordinary functioning of the (spatial) bodily, (sentient) feeling, and narrative senses of self. Selective engagement of the left insula would imply that in this case attempted or actual physiological control is directed toward parasympathetic nervous system activity. Based upon the role of gamma band signaling in driving revision of predictions in hierarchical Bayesian inference models of neural computation (Chao, Takaura, Wang, Fujii, & Dehaene, 2018), gamma band integration within this network may be interpreted as part of a process driving the revision of these predictions to restore stability to the functioning of this system and normalize the operation of higher hierarchical self-models.

This interpretation is further supported by the observation corresponding to localized beta changes. Local networks coding current predictions or expectations have been closely linked to beta band oscillations in animal studies and in recent predictive coding accounts (Michalareas et al., 2016). Bottom up prediction errors, encoded by gamma oscillations and transmitted between cortical regions may be expected to drive revision of predictions coded in beta oscillations thereby bringing about a surge in localized beta band activity in these target cell assemblies.

Gamma band power increases observed in higher visual cortices, beginning in P2, may code error signals generated by a "search" for visual percepts, absent in the ganzfeld, with which to constrain interoceptive and proprioceptive predictions in order to reestablish a stable sense of the "physiological" and bodily self (cf. her imagery of safety reported during this period). This would then trigger the cascade of beta, alpha, and theta band activity observed in these regions in P3 and P4. This process may be linked to Z's high hypnotizability, which we propose enables her to generate perceptual priors in the face of imprecise ganzfeld sensory signals (cf. Acunzo, Cardeña, & Terhune, 2020).

This paper has a number of limitations that should be taken into consideration. Foremost, it is a case study of a single evaluation, with the concomitant statistical and generalizability constraints. Nonetheless, we consider that given the lack of currently available information on spontaneous depersonalization episodes, it can be the source of further hypotheses to be tested with other designs. Second, we used Brodmann area (BA) centroids as ROI in our connectivity analysis. Given that some Brodmann areas are quite large and there is internal functional differentiation, a more fine-grained parcellation of cortical regions may be informative. And given our speculations about the relation of cardiac activity and EEG in this phenomenon, it would have been very useful to have had an electrocardiogram (ECG).

Future investigations should consider using provocation studies targeting the amygdalae and evaluating the role of other frequency bands, particularly in relation to the orchestration of gamma band synchronization. It will be important to consider the role of the left insula (versus right) in functional networks involved in dissociation and to co-record ECG, and perhaps other psychophysiological measures. Naturally occurring events, even if unfortunate ones as in this case, can nonetheless enhance our understanding of the relation between dissociative processes and brain functioning.

CRediT authorship contribution statement

Graham Jamieson: Conceptualization, Data curation, Formal analysis, Visualization. **Etzel Cardeña:** Data curation, Conceptualization, Formal analysis, Funding acquisition, Investigation, Methodology, Project administration, Supervision. **Vilfredo de Pascalis:** Conceptualization.

Data availability

The data that has been used is confidential.

Acknowledgement

The author(s) gratefully acknowledge Lund University Humanities Lab for the use of its EEG facility.

References

Acunzo, D., Cardeña, E., & Terhune, D. B. (2020). Anomalous experiences are more prevalent among highly suggestible individuals who are also highly dissociative. *Cognitive Neuropsychiatry, 25*(3), 179–189. https://doi.org/10.1080/13546805.2020.1715932

Babo-Rebello, M., Richter, C. G., & Tallon-Baudry, C. (2016). Neural responses to heartbeats in the default network encodes the self in spontaneous thoughts. *The Journal of Neuroscience, 36*(30), 7829–7840.

Barrett, L. F., & Simmons, W. K. (2015). Interoceptive predictions in the brain. *Nature Reviews. Neuroscience, 16*(7), 419–429. https://doi.org/10.1038/nrn3950

Biduła, S. P., & Króliczak, G. (2015). Structural asymmetry of the insula is linked to the lateralization of gesture and language. *The European Journal of Neuroscience, 41*(11), 1438–1447. https://doi.org/10.1111/ejn.12888

Brown, S. R. (2009). Reentrant emergence. *American Philosophical Quarterly, 46*(3), 225–238. https://www.jstor.org/stable/40606919.

Carlson, E. B., Waelde, L. C., Palmieri, P. A., Macia, K. S., Smith, S. R., & McDade-Montez, E. (2018). Development and validation of the Dissociative Symptoms Scale. *Assessment, 25*(1), 84–98. https://doi.org/10.1177/1073191116645904

Cardeña, E. (2005). The phenomenology of deep hypnosis: Quiescent and physically active. *International Journal of Clinical and Experimental Hypnosis, 53*(1), 37–59. https://doi.org/10.1080/00207140490914234

Cardeña, E., & Carlson, E. (2011). Acute stress disorder revisited. *Annual Review of Clinical Psychology, 7*, 245–267. https://doi.org/10.1146/annurev-clinpsy-032210-104502

Cardeña, E., Gušić, S., & Cervin, M. (2022). A network analysis to identify associations between PTSD and dissociation among teenagers. *Journal of Trauma & Dissociation, 23*(4), 432–450. https://doi.org/10.1080/15299732.2021.1989122

Cardeña, E., Jönsson, P., Terhune, D. B., & Marcusson-Clavertz, D. (2013). The neurophenomenology of neutral hypnosis. *Cortex, 49*(2), 375–385. https://doi.org/10.1016/j.cortex.2012.04.001

Chao, Z. C., Takaura, K., Wang, L., Fujii, N., & Dehaene, S. (2018). Large-scale cortical networks for hierarchical prediction and prediction error in the primate brain. *Neuron, 100*(5), 1252–1266. https://doi.org/10.1016/j.neuron.2018.10.004

Cooper, J. O., Heron, T. E., & Heward, W. L. (2020). *Applied Behavior Analysis*. UK: Pearson.

Council, J. (1999). Measures of hypnotic responding. In I. Kirsch, A. Capafons, E. Cardeña-Buelna, & S. Amigó (Eds.), *Clinical Hypnosis and Self-Regulation: Cognitive Behavioral Perspectives* (pp. 119–140). Washington: American Psychological Association.

Craig, A. D. (2005). Forebrain emotional asymmetry: A neuroanatomical basis? *Trends in Cognitive Sciences, 9*(12), 566–571. https://doi.org/10.1016/j.tics.2005.10.005

Craig, A. D. (2010). The sentient self. *Brain Structure and Function, 214*, 563–577. https://doi.org/10.1007/s00429-010-0248-y

Derogatis, L. R. (1975). Brief Symptom Inventory. *Clinical Psychometric Research*.

Etkin, A., Egner, T., & Kalisch, R. (2011). Emotional processing in anterior cingulate and medial prefrontal cortex. *Trends in Cognitive Sciences, 15*(2), 85–93. https://doi.org/10.1016/j.tics.2010.11.004

Fuchs, M., Kastner, J., Wagner, M., Hawes, S., & Ebersole, J. S. (2002). A standardized boundary element method volume conductor model. *Clinical Neurophysiology, 113*(5), 702–712. https://doi.org/10.1016/S1388-2457(02)00030-5

Hayashi, K., Makino, M., Hashizume, M., Nakano, K., & Tsuboi, K. (2010). Electroencephalogram abnormalities in panic disorder patients: A study of symptom characteristics and pathology. *Biopsychosoc Med, 4*(9). https://doi.org/10.1186/1751-0759-4-9

Herrmann, C. S., & Debener, S. (2008). Simultaneous recording of EEG and BOLD responses: A historical perspective. *International Journal of Psychophysiology, 67*(3), 161–168. https://doi.org/10.1016/j.ijpsycho.2007.06.006

Hollander, E., Carrasco, J. L., Mullen, L. S., Trungold, S., DeCaria, C. M., & Towey, J. (1992). Left hemispheric activation in depersonalization disorder: A case report. *Biological Psychiatry, 31*(11), 1157–1162. https://doi.org/10.1016/0006-3223(92)90161-r

Kim, J., & Jeong, B. (2019). Heartbeat induces a cortical theta-synchronized network in the resting state. *eNeuro, 6*(4). https://doi.org/10.1523/ENEURO.0200-19.2019

Kirsch, I., Council, J. R., & Wickless, C. (1990). Subjective scoring for the Harvard Group Scale of Hypnotic Susceptibility, Form A. *The International Journal of Clinical and Experimental Hypnosis, 38*, 112–124.

Lachaux, J. P., Fonlupt, P., Kahane, P., Minotti, L., Hoffmann, D., Bertrand, O., & Baciu, M. (2007). Relationship between task-related gamma oscillations and BOLD signal: New insights from combined fMRI and intracranial EEG. *Human Brain Mapping, 28*(12), 1368–1375. https://doi.org/10.1002/hbm.20352

Lanius, R. A., Vermetten, E., Loewenstein, R. J., Brand, B., Schmahl, C., Bremner, J. D., & Spiegel, D. (2010). Emotion modulation in PTSD: Clinical and neurobiological evidence for a dissociative subtype. *American Journal of Psychiatry, 167*(6), 640–647. https://doi.org/10.1176/appi.ajp.2009.09081168

Lanius, R. A., Boyd, J. E., McKinnon, M. C., Nicholson, A. A., Frewen, P., Vermetten, E., … Spiegel, D. (2018). A review of the neurobiological basis of trauma-related dissociation and its relation to cannabinoid- and opioid-mediated stress response: A transdiagnostic, translational approach. *Current Psychiatry Reports, 20*(12), 118. https://doi.org/10.1007/s11920-018-0983-y

Lebois, L. A. M., Kumar, P., Palermo, C. A., Lambros, A. M., O'Connor, L., Wolff, J. D., … Kaufman, M. L. (2022). Deconstructing dissociation: A triple network model of trauma-related dissociation and its subtypes. *Neuropsychopharmacol, 47*, 2261–2270. https://doi.org/10.1038/s41386-022-01468-1

Lemche, E., Anilkumar, A., Giampietro, V. P., Brammer, M. J., Surguladze, S. A., Lawrence, N. S., … Phillips, M. L. (2008). Cerebral and autonomic responses to emotional facial expressions in depersonalisation disorder. *The British Journal of Psychiatry, 193*(3), 222–228. https://doi.org/10.1192/bjp.bp.107.044263

Locatelli, M., Bellodi, L., Perna, G., & Scarone, S. (1993). EEG power modifications in panic disorder during a temporolimbic activation task: Relationships with temporal lobe clinical symptomatology. *The Journal of Neuropsychiatry and Clinical Neurosciences, 5*(4), 409–414. https://doi.org/10.1176/jnp.5.4.409

Marco-Pallarés, J., Grau, C., & Ruffini, G. (2005). Combined ICA-LORETA analysis of mismatch negativity. *NeuroImage, 25*(2), 471–477. https://doi.org/10.1016/j.neuroimage.2004.11.028

Mazziotta, J., Toga, A., Evans, A., Fox, P., Lancaster, J., Zilles, K., … Holmes, C. (2001). A probabilistic atlas and reference system for the human brain: International Consortium for Brain Mapping (ICBM). *Philosophical Transactions of the Royal Society of London. Series B: Biological Sciences, 356*(1412), 1293–1322. https://doi.org/10.1098/rstb.2001.0915

Michalareas, G., Vezoli, J., Van Pelt, S., Schoffelen, J. M., Kennedy, H., & Fries, P. (2016). Alpha-beta and gamma rhythms subserve feedback and feedforward influences among human visual cortical areas. *Neuron, 89*(2), 384–397. https://doi.org/10.1016/j.neuron.2015.12.018

Mobbs, D., Marchant, J. L., Hassabis, D., Seymour, B., Tan, G., Gray, M., … Frith, C. D. (2009). From threat to fear: The neural organization of defensive fear systems in humans. *The Journal of Neuroscience, 29*(39), 12236–12243. https://doi.org/10.1523/JNEUROSCI.2378-09.2009

Molnar-Szakacs, I., & Uddin, L. Q. (2022). Anterior insula as a gatekeeper of executive control. *Neuroscience & Biobehavioral Reviews, 139*, Article 104736. https://doi.org/10.1016/j.neubiorev.2022.104736

Nichols, T. E., & Holmes, A. P. (2002). Nonparametric permutation tests for functional neuroimaging: A primer with examples. *Human Brain Mapping, 15*(1), 1–25. https://doi.org/10.1002/hbm.1058

Nolan, H., Whelan, R., & Reilly, R. B. (2010). FASTER: Fully automated statistical thresholding for EEG artifact rejection. *Journal of Neuroscience Methods, 192*(1), 152–162. https://doi.org/10.1016/j.jneumeth.2010.07.015

Oldfield, R. C. (1971). The assessment and analysis of handedness: The Edinburgh inventory. *Neuropsychologia, 9*(1), 97–113. https://doi.org/10.1016/0028-3932(71)90067-4

Pascual-Marqui, R. D. (2002). Standardized low-resolution brain electromagnetic tomography (sLORETA): Technical details. *Methods and Findings in Experimental and Clinical Pharmacology, 24*(Suppl D), 5–12.

Pascual-Marqui, R. D. (2007). Coherence and phase synchronization: Generalization to pairs of multivariate time series, and removal of zerolag contributions. arXiv: 0706.1776. https://doi.org/10.48550/arXiv.0706.1776.

Pascual-Marqui, R. D. (2009). Theory of the EEG inverse problem. In S. Tong, & N. V. Thankor (Eds.), *Quantitative EEG Analysis: Methods and Clinical Applications* (pp. 121–140). Artech.

Pascual-Marqui, R. D., Lehmann, D., Koukkou, M., Kochi, K., Anderer, P., Saletu, B., … Biscay-Lirio, R. (2011). Assessing interactions in the brain with exact low-resolution electromagnetic tomography. *Philosophical Transactions of the Royal Society A: Mathematical, Physical and Engineering Sciences, 369*(1952), 3768–3784. https://doi.org/10.1098/rsta.2011.0081

Park, H. D., Bernasconi, F., Salomon, R., Tallon-Baudry, C., Spinelli, L., Seeck, M., … Blanke, O. (2018). Neural sources and underlying mechanisms of neural responses to heartbeats, and their role in bodily self-consciousness: An intracranial EEG study. *Cerebral Cortex, 28*(7), 2351–2364. https://doi.org/10.1093/cercor/bhx136

Park, H. D., & Blanke, O. (2019). Heartbeat-evoked cortical responses: Underlying mechanisms, functional roles, and methodological considerations. *NeuroImage, 197*, 502–511. https://doi.org/10.1016/j.neuroimage.2019.04.081

Raimo, E. B., Roemer, R. A., Moster, M., & Shan, Y. (1999). Alcohol-induced depersonalization. *Biological Psychiatry, 45*(11), 1523–1526. https://doi.org/10.1016/S0006-3223(98)00257-1

Reinders, A. A., Willemsen, A. T., den Boer, J. A., Vos, H. P., Veltman, D. J., & Loewenstein, R. J. (2014). Opposite brain emotion-regulation patterns in identity states of dissociative identity disorder: A PET study and neurobiological model. *Psychiatry Research, 223*(3), 236–243. https://doi.org/10.1016/j.pscychresns.2014.05.005

Renaud, K. J. (2015). Vestibular function and depersonalization/derealization symptoms. *Multisensory Research, 28*(5–6), 637–651. https://doi.org/10.1163/22134808-00002480

Roydeva, M. I., & Reinders, A. A. T. S. (2021). Biomarkers of pathological dissociation: A systematic review. *Neuroscience and Biobehavioral Reviews, 123*, 120–202. https://doi.org/10.1016/j.neubiorev.2020.11.019

Salami, A., Andreu-Perez, J., & Gillmeister, H. (2020). Symptoms of depersonalisation/derealisation disorder as measured by brain electrical activity: A systematic review. *Neuroscience and Biobehavioral Reviews, 118*, 524–537. https://doi.org/10.1016/j.neubiorev.2020.08.011

Schäflein, E., Mertens, Y., Lejko, N., Beutler, S., Sattel, H., & Sack, M. (2022). Altered frontal electroencephalography as a potential correlate of acute dissociation in dissociative disorders: Novel findings from a mirror confrontation study. *BJPsych Open, 8*(6), E196. https://doi.org/10.1192/bjo.2022.593

Schauer, M., & Elbert, T. (2010). Dissociation following traumatic stress. *Journal of Psychology, 218*(2), 109–127. https://doi.org/10.1027/0044-3409/a000018

Scheeringa, R., Fries, P., Petersson, K. M., Oostenveld, R., Grothe, I., Norris, D. G., … Bastiaansen, M. C. (2011). Neuronal dynamics underlying high-and low-frequency EEG oscillations contribute independently to the human BOLD signal. *Neuron, 69*(3), 572–583. https://doi.org/10.1016/j.neuron.2010.11.044

Schimmenti, A., & Sar, V. (2019). A correlation network analysis of dissociative experiences. *Journal of Trauma & Dissociation, 20*(4), 402–419. https://doi.org/10.1080/15299732.2019.1572045

Schulz, A., Köster, S., Beutel, M. E., Schächinger, H., Vögele, C., Rost, S., … Michal, M. (2015). Altered patterns of heartbeat-evoked potentials in depersonalization/derealization disorder: Neurophysiological evidence for impaired cortical representation of bodily signals. *Psychosomatic Medicine, 77*(5), 506–516. https://doi.org/10.1097/PSY.0000000000000195

Sedeño, L., Couto, B., Melloni, M., Canales-Johnson, A., Yoris, A., Baez, S., … Ibanez, A. (2014). How do you feel when you can't feel your body? Interoception, functional connectivity and emotional processing in depersonalization-derealization disorder. *PloS one, 6*, Article e98769. https://doi.org/10.1371/journal.pone.0098769

Shor, R. E., & Orne, E. C. (1962). *Harvard Group Scale of Hypnotic Susceptibility: Form A*. Palo Alto, CA: Consulting Psychologists Press.

Simeon, D., Guralnik, O., Hazlett, E. A., Spiegel-Cohen, J., Hollander, E., & Buchsbaum, M. S. (2000). Feeling unreal: A PET study of depersonalization disorder. *American Journal of Psychiatry, 157*(11), 1782–1788. https://doi.org/10.1176/appi.ajp.157.11.1782

Vinck, M., Uran, C., Spyropoulos, G., Onorato, I., Broggini, A. C., Schneider, M., & Canales-Johnson, A. (2023). Principles of large-scale neural interactions. *Neuron, 111*(7), 987–1002. https://doi.org/10.1016/j.neuron.2023.03.015

Wackermann, J., Pütz, P., & Allefeld, C. (2008). Ganzfeld-induced hallucinatory experience, its phenomenology and cerebral electrophysiology. *Cortex, 44*(10), 1364–1378. https://doi.org/10.1016/j.cortex.2007.05.003

Weitzenhoffer, A. M., & Hilgard, E. R. (1962). *Stanford Hypnotic Susceptibility Scale, Form C*. Palo Alto, CA: Consulting Psychologists Press.